Available online at www.sciencedirect.com
ScienceDirect
Trans. Nonferrous Met. Soc. China 32(2022) 2403−2413
Transactions of Nonferrous Metals Society of China
www.tnmsc.cn

Effect of B_2O_3 content on viscosity and structure of SiO_2−MgO−FeO-based slag

Xin-yi ZHANG, Xiao-ming LI, Xiang-dong XING

School of Metallurgical Engineering, Xi'an University of Architecture and Technology, Xi'an 710055, China

Received 12 July 2021; accepted 31 December 2021

Abstract: The effect of B_2O_3 content on the viscosity of SiO_2−MgO−FeO-based molten slag system was investigated using the rotating cylinder method. The evolution process of the melt structure under different contents of B_2O_3 was comprehensively studied via FTIR spectroscopy and a model for calculating the degree of polymerization was developed. The results showed that the viscosity of the molten slag decreased with the addition of B_2O_3, which had a slight effect when its content exceeded 3 wt.%. As the addition of B_2O_3 increased from 0 to 4 wt.%, the break temperature of the slags decreased from 1152 to 1050 °C and the apparent activation energy decreased from 157.90 to 141.84 kJ/mol. The addition of B_2O_3 to the molten slag destroyed the chain silicate structure to form a more cyclic borosilicate structure. The Urbain model was improved to calculate the viscosity of the SiO_2−MgO−FeO-based slags, and the values were in good agreement with the experimentally measured values.

Key words: B_2O_3 content; molten slag; viscosity; activation energy; structure

1 Introduction

As an important strategic metal, nickel is produced mainly from nickel sulfide ore. With the gradual consumption of high-grade nickel sulfide ore, the low-grade ore with a high magnesia content has gradually become a possible raw material for nickel smelting. The magnesia will change the melting point and viscosity of the slag, which makes the increase of the operation difficulty of nickel flash furnace smelting process. Currently, the MgO content of the flash furnace slag used in Jinchuan Company, China, is approximately 10 wt.%. To keep the slag viscosity within a reasonable range for smelting, the temperature needs to be increased significantly corresponding to the small increase of MgO in the nickel ore, which leads to a quick increase of smelting energy consumption, and the production costs of the company will increase. Therefore, in this work a way of adding B_2O_3 was proposed to improve viscous flow characteristics of the slag, reduce the smelting temperature, and achieve the goal of saving energy during nickel flash furnace melting.

Previous research proved that a small amount of B_2O_3 could remarkably enhance the fluidity of slag. WEI et al [1] found that the break temperature of fluorine-free mold fluxes was reduced with the addition of B_2O_3. WANG et al [2] studied the effects of B_2O_3 on the rheological behavior of MgO−SiO_2-based slag, which suggested that the viscosity of the slag decreased with the increase of B_2O_3 content from 3 wt.% to 9 wt.%. It was also observed that although B_2O_3 was a maker, it still could reduce the viscosity of the fluoride-free slag [3]. To evaluate the effect of B_2O_3 on the viscous flow characteristics of molten slag, the break temperature [4,5], activation energy [6], structure [7−10] and viscosity prediction model [11]

Corresponding author: Xiao-ming LI, Tel: +86-18702982898, E-mail: xmli88@126.com;
Xiang-dong XING, Tel: +86-15686259876, E-mail: xaxxd@xauat.edu.cn
DOI: 10.1016/S1003-6326(22)65956-9
1003-6326/© 2022 The Nonferrous Metals Society of China. Published by Elsevier Ltd & Science Press

of molten slag have been studied extensively. However, these studies mainly focused on the two types of slag systems, such as blast furnace slag and continuous casting protection slag. Up to now, the precise effect on nickel flash melting furnace slag containing a high MgO content and a high FeO content has not been systematically investigated. The presence of large amounts of basic oxides may change the form of the main silicate structure of the melt, and the effect of B_2O_3 on the structure should also be revealed. In addition, about 3 wt.% of other components, such as CaO and Al_2O_3, may also be present in the nickel flash molten slag, but their action mechanism is unclear. Therefore, studying the viscosity and structure of SiO_2−MgO−FeO-based slag is of great significance for making full use of nickel ore with high magnesium contents.

In this study, rotating cylinder method was adopted to measure the viscosity of a SiO_2−MgO−FeO-based slag system with varying B_2O_3 contents. The structural transformation was investigated by Fourier transform infrared (FTIR) spectroscopy and verified by calculating the break temperature and apparent activation energy. The influence mechanism of B_2O_3 in SiO_2−MgO−FeO-based nickel flash molten slag was determined and discussed.

2 Experimental

2.1 Materials

The experimental samples were prepared based on the actual slag from the smelting of high-MgO nickel sulfide ore in a flash furnace, and the main components were FeO, MgO, SiO_2, Al_2O_3 and CaO [12]. To avoid the influence of trace elements in the actual slag sample, an analytically pure reagent was used to prepare the experimental slag sample. The FeO in the experimental samples was obtained from FeC_2O_4. The contents of B_2O_3 were 0, 1, 2, 3 and 4 wt.%, respectively. The compositions of the samples are shown in Table 1. A given amount of chemical reagent was precisely weighed and then put into a vertical tube furnace and heated at 1500 °C for 180 min in an argon (99.999%, 0.3 L/min) atmosphere to make the chemical composition uniform. The pre-melted sample was poured into water to obtain a completely glassy phase, and the glass-like sample was then crushed. All slag samples were tested by X-ray diffraction (XRD, D8 ADVANCE A25; Bruker AXS, Germany) to confirm that the molten slag after quenching was amorphous. The main chemical contents of the sample determined using X-ray fluorescence spectrometry (XRF, S4 Explorer, Bruker, Germany) are shown in Table 1. Finally, Fourier transform infrared (FTIR) spectroscopy (Thermo Fisher; Nicolet iS5) was performed on pre-melted slag samples to explore the effect of B_2O_3 on the structure of nickel slag.

2.2 Viscosity measurements

The viscosities of the samples were measured using a viscometer (RTW−10, Northeastern University, China). The equipment used for the experiments is shown in Fig. 1. The viscometer was calibrated using castor oil before each viscosity measurement. During the viscosity measurement, the experimental samples (150 g) were placed in a Pt crucible (inner diameter of 50 mm and height of 70 mm). The samples were heated to 1500 °C at a rate of 5 °C/min and maintained at that temperature for approximately 240 min to ensure that the temperature and composition of the molten slag were uniform. Then, spindle (Mo, diameter of 15 mm) was infused into the fluid slag slowly with a low rotation rate, and the slag was cooled slowly to 1320 °C and held at a certain temperature for

Table 1 Experimental compositions of slags (wt.%)

No.	Pre-experimental composition (weighed)						No.	Post-experimental composition (XRF)					
	CaO	FeO	SiO_2	Al_2O_3	MgO	B_2O_3		CaO	FeO	SiO_2	Al_2O_3	MgO	B_2O_3
1	1.2	52.76	34.04	2.3	9.7	0	1	1.33	52.82	34.02	2.13	9.86	0
2	1.2	52.15	33.65	2.3	9.7	1	2	1.28	52.21	33.51	2.09	9.89	0.92
3	1.2	51.55	33.25	2.3	9.7	2	3	1.31	51.66	33.01	2.11	9.91	1.79
4	1.2	50.94	32.86	2.3	9.7	3	4	1.33	51.03	32.63	2.14	9.85	2.89
5	1.2	50.33	32.47	2.3	9.7	4	5	1.35	50.45	32.26	2.19	9.81	3.86

10 min to ensure that it was uniform and stable. The viscosity value was calculated and recorded by the software on the computer. The experimental profile for the viscosity measurement is shown in Fig. 2.

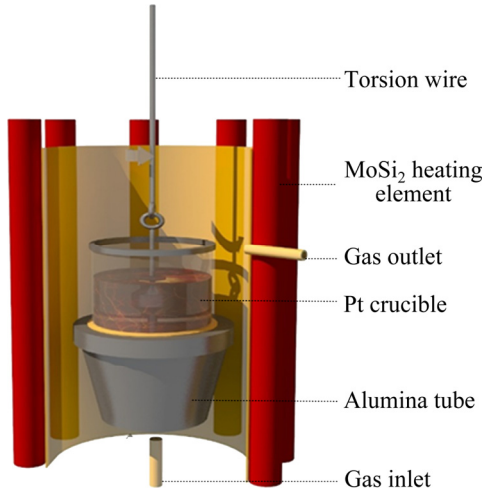

Fig. 1 Schematic diagram of experimental apparatus

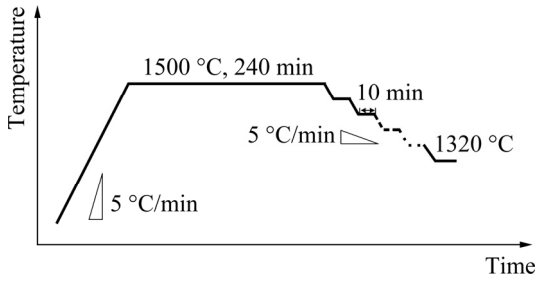

Fig. 2 Temperature regime curve for viscosity experiment

3 Results

3.1 Effect of B_2O_3 content on melt viscosity

The viscosities of samples with varying B_2O_3 contents at different temperatures are shown in Fig. 3. Under the condition of the temperatures between 1100 and 1350 °C, the viscosity decreased as the B_2O_3 content increased from 0 to 4 wt.%. When the B_2O_3 content increased from 0 to 3 wt.%, the viscosity of the molten slag decreased rapidly, and the effect on the viscosity was relatively slightly with further increase of the B_2O_3 content. It was deduced that there was a moderate content of B_2O_3 to improve the viscosity of the SiO_2−MgO−FeO-based molten slag.

3.2 Break temperature and apparent activation energy

The break temperature (T_{br}) can be represented by the intersection of the viscosity−temperature curve and a 45° tangent line, representing the temperature at which the viscosity changes significantly [2]. It is a key parameter to determine the rheological behavior of nickel slags. T_{br} values of Samples 1, 2, 3, 4 and 5 with B_2O_3 contents of 0, 1, 2, 3 and 4 wt.% were 1152, 1130, 1107, 1075 and 1050 °C, respectively, as shown in Fig. 4. Sample 1 (without B_2O_3) had the highest T_{br} (1152 °C), which would decrease continuously as the addition of B_2O_3 increased. This is mainly due to the fact that B_2O_3 is one kind of fluxing agent which could decrease the liquidus temperature of slag. On the other hand, this tendency seems to be related to a shift from a silicate network structure to a borosilicate network structure [7,13].

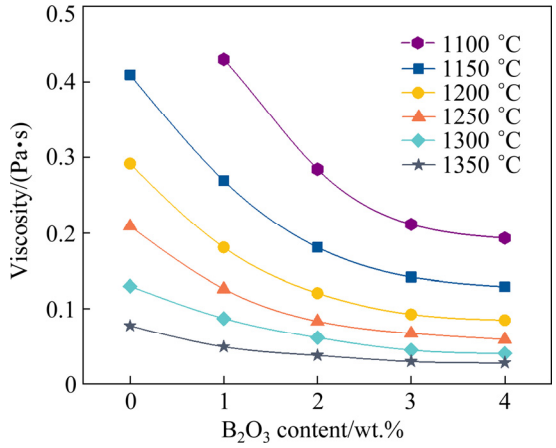

Fig. 3 Viscosity of molten slags with varying B_2O_3 contents

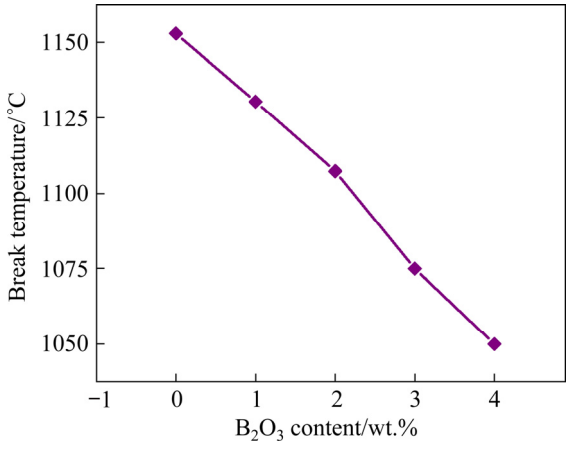

Fig. 4 Variation in break temperature of nickel slags with varying B_2O_3 content

As an important viscous property of molten slags, the viscous flow activation energy could reflect the resistance when the viscous flow unit should overcome to move between different equilibria, which could also reveal changes in the

molten slag structure [5,14]. The viscous flow activation energy can be calculated according to the Arrhenius equation shown as follows:

$$\eta=A\exp[E_a/(RT)] \quad (1)$$

where η represents the viscosity of the molten slag (Pa·s); A is the pre-exponent factor; R is the molar gas constant (8.314 J/(mol·K)); E_a stands for the activation energy of the molten slag (kJ/mol), and T means the thermodynamic temperature (K).

The logarithm of Eq. (1) is taken to obtain Eq. (2):

$$\ln\eta=\ln A+E_a/(RT) \quad (2)$$

The fitting relationship between the natural logarithm of the viscosity ($\ln\eta$) and $1/T$ is shown in Fig. 5. The apparent activation energy (E_a) of the slag can be obtained from the slope of the fitted straight line, which is plotted in Fig. 6. With the increase of B_2O_3 content from 0 to 4 wt.%, the viscous flow activation energy of the slag samples decreased from 157.90 to 141.84 kJ/mol. The increase in B_2O_3 content reduces the barrier to flow and the viscosity of the molten slag, which is consistent with the viscosity measurements. The change in the activation energy reflects the transformation of the molten flow unit, which means that adding B_2O_3 can change the composition of the flow unit of the molten slag [15].

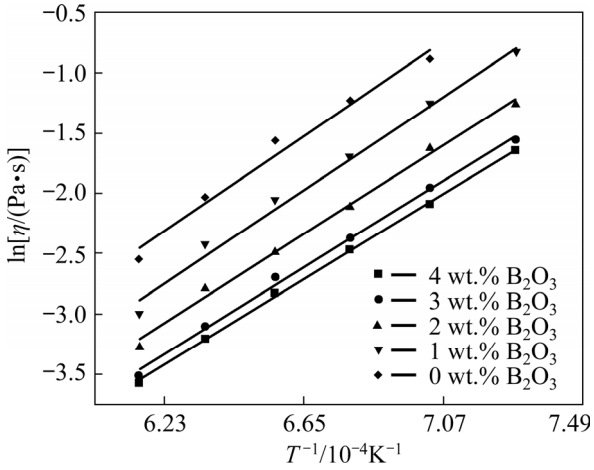

Fig. 5 Plots of $\ln\eta$ versus $1/T$ for molten slag with different B_2O_3 contents

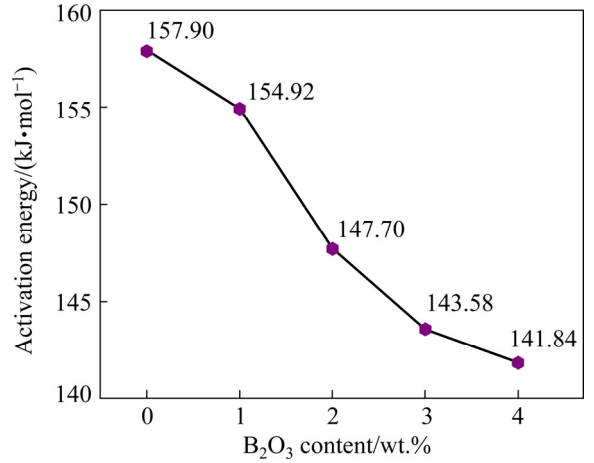

Fig. 6 Calculated apparent activation energies of slag samples with different B_2O_3 contents

3.3 Effect of B_2O_3 on molten slag structure observed using FTIR

The FTIR spectra of the SiO_2−MgO−FeO-based molten slags with various B_2O_3 contents are shown in Fig. 7. The corresponding transmittance regions of infrared (IR) active structural units from recognized references are summarized in Table 2.

The transmittance troughs of the [BO_3] stretching at 1200−1600 cm^{-1} were significantly deeper, and the [BO_3]-trihedral bending vibration band at 700−750 cm^{-1} was enhanced with increasing B_2O_3 content. This indicates that B^{3+} mostly existed in the form of [BO_3] groups in the molten slag system. Meanwhile, the basic metal oxides in the molten slag system provided a large amount of free oxygen ions to form [BO_2O^-]-trihedral bond, which is consistent with previous studies [16,17].

The [SiO_4]-tetrahedral bands were divided into four typical silicate structural units Q^n (n=0, 1, 2, and 3, behalf of the number of bridging oxygen atoms) [18]. In Fig. 7, the molten slag without B_2O_3 contained more Q^2 and less Q^3, Q^0 and Q^1, indicating that the Si—O structure in the molten slag was dominated by chains (Q^2). Compared to conventional silicate molten slag, the basic oxides in the SiO_2−MgO−FeO-based slag system could provide more free oxygen ions, which were easier to form a chain or other simple structure by cutting down intricate silicate network. Depending on the charge balance, the interrupted Si—O—Si structure always connected to a cation, forming a Si—O—M structure [19]. The Q^2 in the [SiO_4]-tetrahedral band decreased substantially, and the Si—O—Si bending vibration (400−600 cm^{-1}) decreased, which means that the original Si—O—Si structural units were depolymerized.

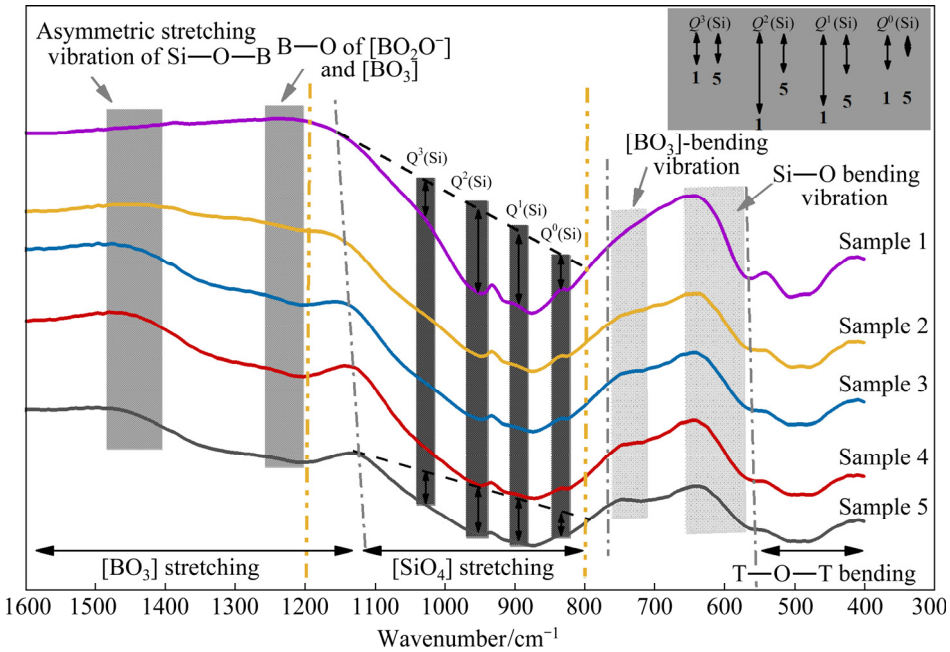

Fig. 7 FTIR results of as-quenched samples with various B_2O_3 contents

Table 2 Assignments of FTIR spectra bands

Wavenumber/ cm^{-1}	Assignment	Ref.
400−600	T—O—T bending vibrations	[14,20,21]
650	Si—O bending vibration	[2,5,22]
700−750	$[BO_3]$ bending vibration	[23]
850	Q^0 ($[SiO_4]^{4-}$ monomers)	[2,5,22]
900	Q^1 ($[Si_2O_7]^{6-}$ dimers)	[2,5,22]
950−1000	Q^2 ($[Si_3O_{10}]^{8-}$ chains)	[2,5,22]
1050	Q^3($[Si_3O_9]^{6-}$ rings)	[2,5,22]
1200−1600	$[BO_3]$-stretching vibration	[14,24,25]
1250	B—O of $[BO_3]$- and $[BO_2O^-]$-trihedral bond	[14,24,25]
1450	Asymmetric stretching vibration of Si—O—B	[2,14,24,25]

T denotes Si, Al, or Ti elements

3.4 Structural analysis results of melt slag using XPS

The FTIR spectra indicated that adding B_2O_3 to the nickel slag had a significant effect on the melt structure. To obtain quantitative results, the main O 1s peaks of the melt structure of samples were analyzed by XPS and the results are illustrated in Fig. 8.

There are three different types of oxygen present in silicate melts, the bridging oxygen (BO), the non-bridging oxygen (NBO) and the free oxygen (FO), respectively. The variation in the fraction of different types of oxygen ions can provide details of the bonding complexity of the melt [26]. Figure 8 shows the binding energies of nearly 530.3, 531.3, and 532.2 eV are assigned to free oxygen, non-bridging oxygen, and bridging oxygen, respectively [27]. And the intensity peaks which correspond to the varying oxygen ion species change appreciably with the addition of B_2O_3. In particular, the non-bridging oxygen is always a relatively large part of the melt, and the fraction of bridging oxygen gradually increases with the increase of B_2O_3 content. It can be observed that, the proportion of bridging oxygen gradually increases, resulting in a higher degree of polymerization (DOP) for the melt [18].

The proportions of BO, NBO and FO can be obtained by calculating the combined area of the deconvolution peaks, which are shown in Fig. 9. When the B_2O_3 content reaches 4 wt.%, the proportion of BO increases from 14.14% to 23.67%, while the proportion of NBO increases from 21.12% to 32.95%. This further suggests that B_2O_3 can link silicate structure in the melt and produce more aggregated BO.

3.5 Degree of polymerization of borosilicate structure

The parameter degree of polymerization (DOP)

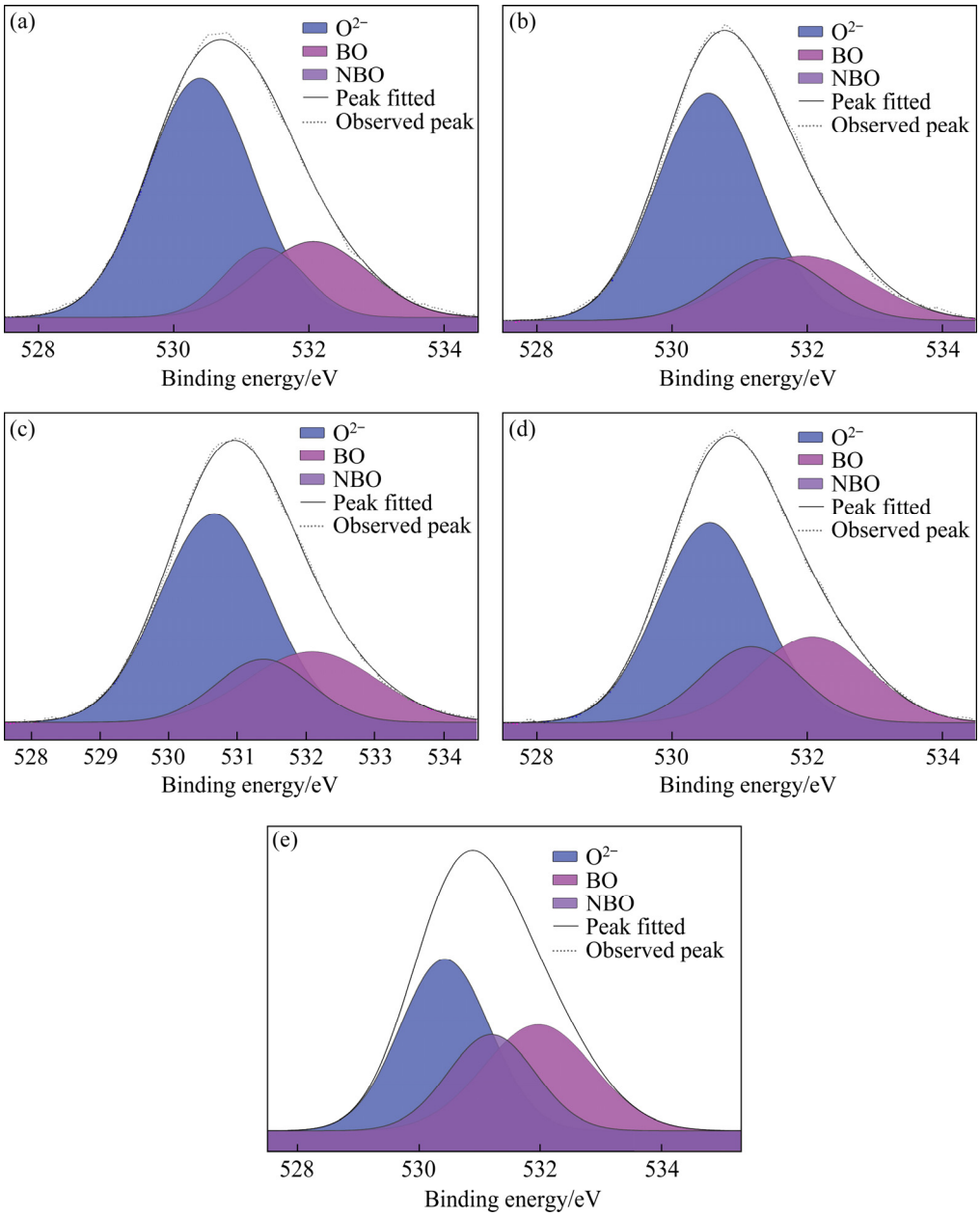

Fig. 8 O 1s XPS spectra for SiO_2−MgO−FeO-based molten slags as function of binding energy with varying B_2O_3 contents: (a) Without B_2O_3; (b) 1 wt.% B_2O_3; (c) 2 wt.% B_2O_3; (d) 3 wt.% B_2O_3; (e) 4 wt.% B_2O_3

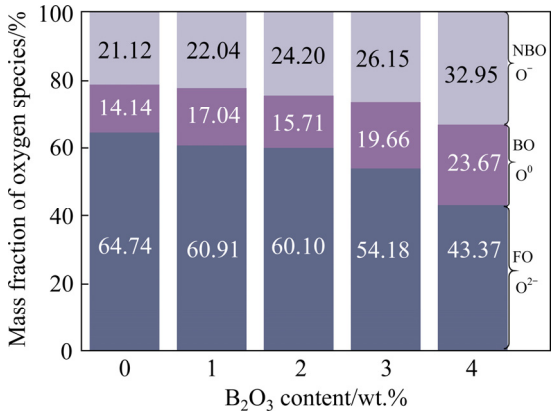

Fig. 9 Proportions of different types of oxygen

represents the structure of the molten slag and has a very strong relationship with the viscosity. In general, the ratio of the molar fraction of the available network breaking oxides to the molar fraction of the tetrahedral coordination cations (F) is used to characterize the DOP, while Q could reflect DOP of the molten slag structure, as shown in Eqs. (3) and (4) [9,21]:

$$F=\frac{2(\sum x_{M_2O}+\sum x_{MO}-x_{Al_2O_3})}{x_{SiO_2}+2x_{Al_2O_3}} \tag{3}$$

$$Q=4-F \tag{4}$$

where MO and M_2O are basic metal oxides and x represents the molar fraction of each component.

In the molten slag systems, CaO, FeO, and MgO are generally considered as network modifiers, and their molar fractions are included in the numerator of Eq. (3). SiO_2 and B_2O_3 usually act as network forming agents, and their mole fractions are put into the denominator of the equation. MIN et al [22] mentioned that Al_2O_3 is an amphoteric oxide for SiO_2−Al_2O_3 molten slag systems, and the Al—O bond can only be detected at mass fraction of Al to (Al + Si) >0.19 wt.%. Otherwise, it is stable as Al^{3+} in the molten slag. In this study, the content of Al_2O_3 (2.3 wt.%) is relatively low compared to that of SiO_2 (from 32.47 wt.% to 34.04 wt.%) and mass fraction of Al to (Al + Si) <0.1 wt.%. In addition, there is no significant $[AlO_4]$ telescopic vibration in the FTIR diagram, suggesting that Al_2O_3 is present in the molten slag as monomeric Al^{3+} ions. Thus, it can be inferred that Al_2O_3 could act as a network breaker, releasing Al^{3+} and O^{2-} ions and breaking the network structure of the present molten slag system. Equations (3) and (4) can be modified as follows:

$$F_1=\frac{2(\sum x_{CaO}+\sum x_{FeO}+\sum x_{MgO}+x_{Al_2O_3})}{x_{SiO_2}+x_{B_2O_3}} \quad (5)$$

$$Q_1=4-F_1 \quad (6)$$

where F_1 and Q_1 are modified values of F and Q, respectively.

In Fig. 10, it is clear that as the B_2O_3 content increases, Q_1 value increases, and the F_1 value decreases, which also indicates an increase in the DOP of the molten slag structure. This result is consistent with the conclusion of the XPS analysis.

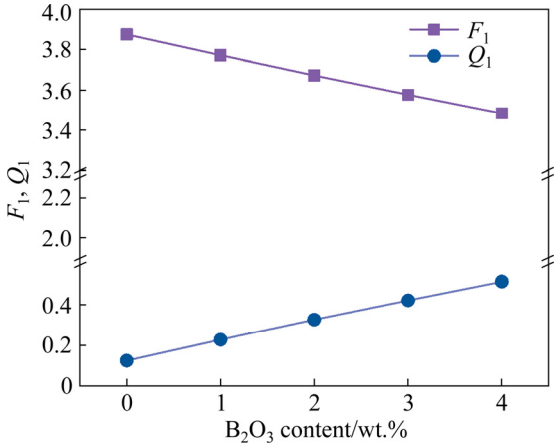

Fig. 10 Changes in F_1 and Q_1

In general, an increase in the DOP leads to increasing the viscosity of the molten slag. However, previous studies on the viscosity of silicate melts have shown that B_2O_3 can effectively reduce viscosity [9,23]. Therefore, the viscosity is not just determined by the DOP of the structural units in the molten slag. Despite DOP changes, it also has other competitive effects to reduce molten slag viscosity which merits further discussion.

4 Discussion

4.1 Evolution of molten slag structure

SiO_2−FeO−MgO-based molten slag systems contain substantial basic oxides of FeO and MgO, which generally act as network modifiers in the molten slag, to release free oxygen ions (O^{2-}). Therefore, the silicate network structure is depolymerized from the mesh into simpler chains ($[Si_2O_7]^{6-}$), as shown in Fig. 11.

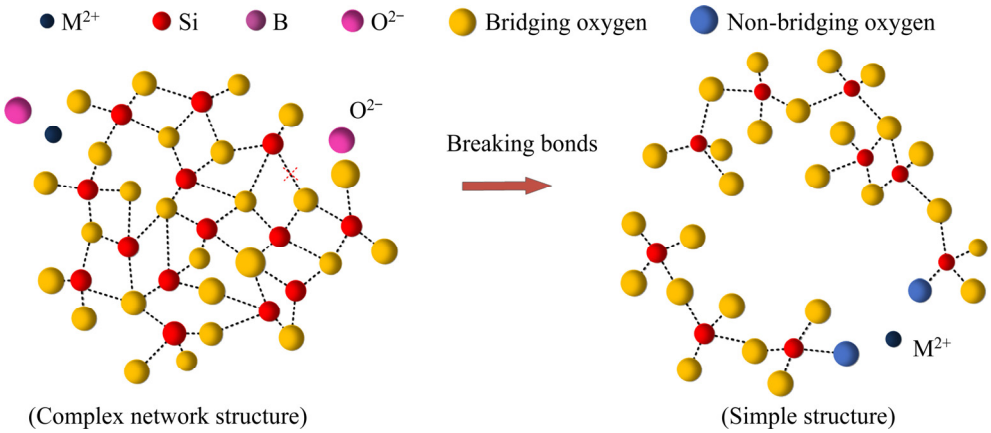

Fig. 11 Decomposition of silicate networks

The addition of B_2O_3 to the molten slag system produces [BO_3]-trihedral structural units. In the presence of a basic oxide (MO), part of the [BO_3]-trihedral units which combine with O^{2-} in the molten slag could form asymmetric [BO_2O^-]-trihedral structures (containing non-bridging oxygen), as shown in Fig. 12, which is close to that observed by WANG et al [28]. The FTIR analysis of the [BO_3] stretching vibration and the B—O bonding vibration bands in the [BO_3]- and [BO_2O^-]-trihedral units become more significant with the addition of B_2O_3, which could also confirm this conclusion.

The [BO_2O^-]- and [BO_3]-trihedral structural units were generated by the combination of B_2O_3 with the chain silicate structures of the molten slag to form more ring-like structures. In this process, the Si—O—Si bonds present in the long chain-like structure are broken, while the ends of the shorter chain-like silicate structure are joined to become the more mobile Si—O—B ring structure. The chains containing [BO_3]- and [BO_2O^-]-trihedral units became more complex than the one without adding B_2O_3, thus increasing the DOP of the molten slag. This explains results from the FTIR analysis, where adding B_2O_3 decreases the bending vibration of Si—O—Si while increasing the Si—O—B asymmetric tensile vibration. And the decrease in the fraction of non-bridging oxygen and an increase in the fraction of bridging oxygen also explained the results of the XPS analysis. The evolution of the molten slag structure during the reaction is schematically shown in Fig. 13.

In general, adding B_2O_3 could improve the melt flow and reduce the melt viscosity, while the melt DOP increases as the following three ways.

In the presence of FeO and MgO, the B—O bonds in the molten slag mainly appear as [BO_2O^-] and [BO_3] two linkage modes [24,25]. As one of the dominant B-related units, the [BO_3]-trihedral unit exhibits a simple two-dimensional (2D) structure that can greatly reduce the viscous resistance during flow [29]. At the same time, the [BO_2O^-]-trihedral structure unit generated in the presence of O^- contains more non-bridging oxygen, which also reduces the symmetry of the molten slag structure. Moreover, WANG and CHOU [30] also suggested that the formation of [BO_2O^-] can decrease the viscosity of molten slag. These factors make [BO_3] as a simple planar structure, reduce the viscosity of slag, and improve the fluidity of slag.

Meanwhile, the B—O trihedral structure is introduced into the silicate network, which disrupts the Si—O—Si structural units and forms

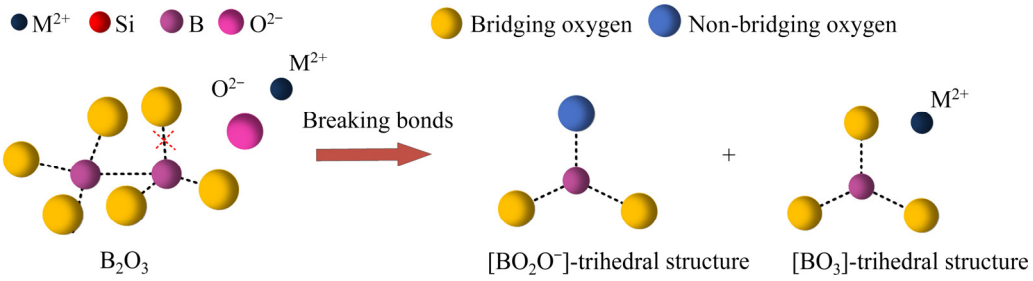

Fig. 12 Decomposition process of B_2O_3

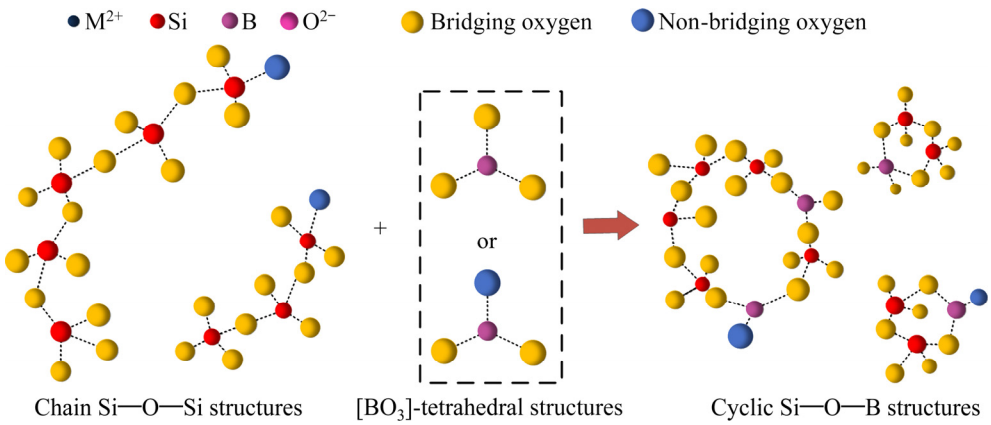

Fig. 13 Decomposition of Si—O—B structures

asymmetric Si—O—B bonds. In addition to reducing the number of less mobile chain structures to generate small and mobile ring structures, and the role of B is also in changing bond energies. The electronegativity of B (2.0) is higher than that of Si (1.8) and attracts more electrons [21]. As a result, the valence electron cloud in Si—O—Si is biased towards the B atom, which weakens the covalent bonds in Si—O. Some Si—O bonds are shortened under the influence of boron oxide, while others grow, which reduces the uniformity of the network and the strength of the structure. This is clearly illustrated by the fact that with the addition of B_2O_3, the Si—O—Si bending vibrations of the molten slag samples in the range of 400−600 cm^{-1} of the FTIR spectrum are reduced.

In addition, as a low-melting oxide (with a melting point of 450 °C), B_2O_3 could combine with oxides in the molten slag to form a series of low-melting compounds, which can significantly reduce the break temperature of the molten slag and increase the superheat of the molten slag system [2,8]. Therefore, in previous studies, the molten slag viscosity decreased with increasing B_2O_3 content in the borosilicate melt.

4.2 Models and prediction of viscosity

The rotating cylinder method is widely used in molten slag viscosity measurements. However, it is difficult to apply the method to actual production because of the complex and variable composition. Numerous viscosity models have been developed over a long period to predict the viscosity of metallurgical molten slag over a range of components and temperatures, for example, URBAIN [31] and IIDA et al [32]. Among them, the Urbain model provides good predictions for conventional SiO_2−MO and its subsystems, with a wide application range. KONDRATIEV and JAK [11] have also corrected the Urbain model and applied it to the SiO_2−Al_2O_3−CaO−FeO quaternion. The Urbain model is a two-parameter expression for viscosity and can be expressed as follows:

$$\eta=A^*T\exp(1000B/T) \tag{7}$$

In this work, the Urbain model is modified to describe the viscosity behaviour of all-liquid molten slags with relatively high concentrations of basic oxides, such as FeO. The new model reclassifies the oxides according to the molten slag situation and optimizes parameter B to classify all cations into three categories: network forming agents, modifiers and amphiphilic cations, as follows:

Network forming agents: $x_G=x_{SiO_2}+x_{B_2O_3}$;

Network modifier: $x_M=x_{CaO}+x_{MgO}$;

Amphoteric: $x_A=x_{Al_2O_3}$.

where A^* is a modified pre-exponential parameter; B is a parameter related to x_G, x_M, and x_A; x_A, x_M and x_G are the mole fractions of the network forming agents, network modifier oxides and amphoteric oxides, respectively.

The relation between A^* and B can be calculated by as follows:

$$-\ln A^*=mB+n \tag{8}$$

$$B=B_0+B_1x_G+B_2x_G^2+B_3x_G^3 \tag{9}$$

$$B_i=a_i+b_i\alpha+c_i\alpha^2 \tag{10}$$

$$\alpha=\frac{\sum x_M}{\sum x_M+x_A} \tag{11}$$

where a_i, b_i and c_i (i=0, 1, 2, and 3) are the coefficients obtained by fitting the experimental data.

Since the empirical parameters m and n proposed by Urbain could not accurately estimate the values of A^* and B, the parameters m and n are obtained from the experimental data. Figure 14 shows the relationship between $-\ln A^*$ and B, and the model corrected for linear fit is used with m=0.301 and n=16.474. The viscosity values obtained from Eqs. (7) and (8) are compared with the experimental data, as shown in Fig. 15.

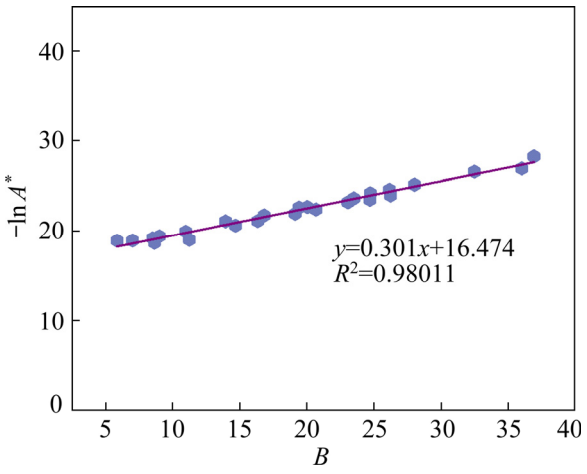

Fig. 14 Relationship between $-\ln A^*$ and B

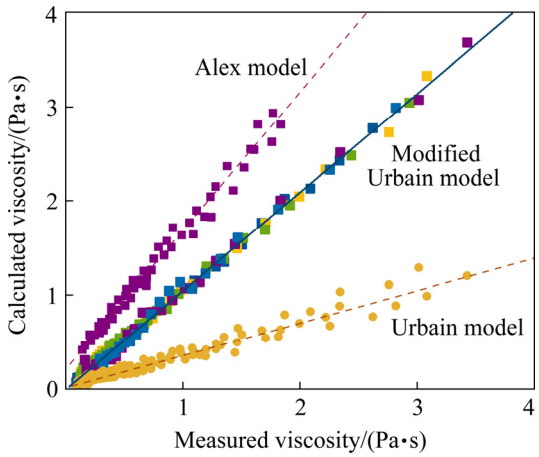

Fig. 15 Comparison of viscosities estimated by modified model with measured values

The viscosity values measured in this investigation are in great agreement with the calculated viscosity values, while the estimated values of the Urbain model and the modified model by Alex differ greatly from the actual measured values, as shown in Fig. 15. To examine the prediction effect, the mean deviation ($\bar{\Delta}$) can be calculated by Eq. (12):

$$\bar{\Delta}=\frac{1}{5}\sum_{N=1}^{5}\frac{\left|\eta_N^{\text{calculated}}-\eta_N^{\text{measured}}\right|}{\eta_N^{\text{measured}}} \tag{12}$$

where η_N^{measured} and $\eta_N^{\text{calculated}}$ are the measured and calculated values of the viscosity, respectively, and N is the number of experimental samples.

The average deviation calculated by the modified new model is small and approximately 15.8%.

5 Conclusions

(1) The viscosity of the SiO_2−MgO−FeO-based slag decreased with the addition of B_2O_3. When the added B_2O_3 content was greater than 3 wt.%, the effect of the addition amount on the viscosity of the slag decreased.

(2) The break temperatures and apparent activation energies of slag samples decreased with increasing B_2O_3 content. The break temperatures were 1152, 1130, 1107, 1075 and 1050 °C when B_2O_3 of 0, 1, 2, 3 and 4 wt.% was added, respectively, and the apparent activation energy of the slags decreased from 157.90 to 141.84 kJ/mol when 4 wt.% B_2O_3 was added.

(3) The addition of B_2O_3 to the molten slag destroyed the chain silicate structure and formed more mobile Si−O−B cyclic structure units, which results in the decreasing viscosity of slag with the addition of boron oxide.

(4) The modified Urbain model can be used to predict the viscosity of SiO_2−MgO−FeO-based slags with a calculated average deviation of about 15.8%.

Acknowledgments

The present work was financially supported by the National Natural Science Foundation of China (No. 51774224).

References

[1] WEI Juan, WANG Wan-lin, ZHOU Le-jun, HUANG Dao-yuan, ZHAO Huan, MA Fan-jun. Effect of Na_2O and B_2O_3 on the crystallization behavior of low fluorine mold fluxes for casting medium carbon steels [J]. Metallurgical and Materials Transactions B, 2014, 45(2): 643−652.

[2] WANG Wan-lin, DAI Shi-fan, ZHOU Le-jun, ZHANG Jian-kang, TIAN Wei-guang, XU Jia-lin. Viscosity and structure of MgO−SiO_2-based slag melt with varying B_2O_3 content [J]. Ceramics International, 2020, 46(3): 3631−3636.

[3] ZHANG Lei, WANG Wan-lin, XIE Sen-lin, ZHANG Kai-xuan, SOHN I. Effect of basicity and B_2O_3 on the viscosity and structure of fluorine-free mold flux [J]. Journal of Non-Crystalline Solids, 2017, 460: 113−118.

[4] SUN Yong-qi, LIAO Jun-lin, ZHENG Kai, WANG Xi-dong, ZHANG Zuo-tai. Effect of B_2O_3 on the structure and viscous behavior of Ti-bearing blast furnace slags [J]. JOM, 2014, 66(10): 2168−2175.

[5] GAO Yan-hong, BIAN Ling-tao, LIANG Zhong-yu. Influence of B_2O_3 and TiO_2 on viscosity of titanium-bearing blast furnace slag [J]. Steel Research International, 2015, 86(4): 386−390.

[6] LIN Yin-he, ZHENG Bin, LUO Len-gen, JIA Yu-long, ZHANG Li-qiang. The online research of B_2O_3 on crystal behavior of high Ti-bearing blast furnace slag [J]. Journal of Chemistry, 2019, 2019: 5498325.

[7] LIN Yin-he, WEN Yong-cai, FU Wei-guo, RAO Jia-ting. Effect and mechanism of B_2O_3 on apparent viscosity of slag during smelting of vanadium-titanium magnetite in the blast furnace [J]. Metallurgical Research & Technology, 2016, 113(5): 506.

[8] SHI Yu, WEI Yong-gang, ZHOU Shi-wei, LI Bo, YANG Yin-dong, WANG Hua. Effect of B_2O_3 content on the viscosity of copper slag [J]. Journal of Alloys and Compounds, 2020, 822: 153478.

[9] ZHANG Lei, WANG Wan-lin, ZHAI Bing-yu, SOHN I. The evolution of the mold flux melt structure during the process of fluorine replacement by B_2O_3 [J]. Journal of the American Ceramic Society, 2020, 103(1): 112−121.

[10] YANG Jian, ZHANG Jian-qiang, SASAKI Y, OSTROVSKI O, ZHANG Chen, CAI De-xiang, KASHIWAYA Y. Effect of B_2O_3 on crystallization behavior, structure, and heat transfer of CaO−SiO_2−B_2O_3−Na_2O−TiO_2−Al_2O_3−MgO−Li_2O mold fluxes [J]. Metallurgical and Materials Transactions B, 2017, 48(4): 2077−2091.

[11] KONDRATIEV A, JAK E. Review of experimental data and modeling of the viscosities of fully liquid slags in the Al_2O_3−CaO−'FeO'−SiO_2 system [J]. Metallurgical and Materials Transactions B, 2001, 32(6): 1015−1025.
[12] LI Xiao-ming, ZHANG Xin-yi, ZANG Xu-yuan, XING Xiang-dong. Structure and phase changes of nickel slag in oxidation treatment [J]. Minerals, 2020, 10(4): 313.
[13] BELASHCHENKO D. Computer simulation of the structure and properties of non-crystalline oxides [J]. Russian Chemical Reviews, 1997, 66(9): 733−762.
[14] KIM G H, SOHN I. Role of B_2O_3 on the viscosity and structure in the CaO−Al_2O_3−Na_2O-based system [J]. Metallurgical and Materials Transactions B, 2014, 45(1): 86−95.
[15] ZHANG Guang-zong, WANG Nan, CHEN Min, LI Hui. Viscosity and structure of CaO−SiO_2−"FeO"−Al_2O_3−MgO system during iron-extracting process from nickel slag: Part 1. Coupling effect of "FeO" and Al_2O_3 [J]. Steel Research International, 2018, 89(10): 1800272.
[16] LI Jiang-ling, CHOU Kuo-chi, SHU Qi-feng. Structure and viscosity of CaO−Al_2O_3−B_2O_3 based mould fluxes with varying CaO/Al_2O_3 mass ratios [J]. ISIJ International, 2020, 60(1): 51−57.
[17] DU L S, STEBBINS J F. Network connectivity in aluminoborosilicate glasses: A high-resolution ^{11}B, ^{27}Al and ^{17}O NMR study [J]. Journal of Non-Crystalline Solids, 2005, 351: 3508−3520.
[18] XING Xiang-dong, PANG Zhuo-gang, MO Chuan, WANG Sha, JU Jian-tao. Effect of MgO and BaO on viscosity and structure of blast furnace slag [J]. Journal of Non-Crystalline Solids, 2020, 530: 119801.
[19] SOHN I, MIN D J. A review of the relationship between viscosity and the structure of calcium−silicate-based slags in ironmaking [J]. Steel Research International, 2012, 83(7): 611−630.
[20] LI Peng-cheng, NING Xiao-jun. Effects of MgO/Al_2O_3 ratio and basicity on the viscosities of CaO−MgO−SiO_2−Al_2O_3 slags experiments and modeling [J]. Metallurgical and Materials Transactions B, 2016, 47(1): 446−457.
[21] WANG Hao, CHEN Zi-wei, LIU Li-li, SUN Yong-qi, WANG Xi-dong. Roles of P_2O_5 addition on the viscosity and structure of CaO−SiO_2−Al_2O_3−Na_2O−P_2O_5 melts [J]. ISIJ International, 2018, 58(9): 1644−1649.
[22] MIN Yi, ZHONG Ming, HUANG Jian, LIU Cheng-jun, JIANG Mao-fa. Structural behavior of Al^{3+} in mould flux glasses of CaO−SiO_2−Al_2O_3−Na_2O−CaF_2 system [J]. Steel Research International, 2014, 85(7): 1194−1199.
[23] HU Kai, LV Xue-wei, LI Sheng-ping, LV Wei, SONG Bing, HAN Ke-xi. Viscosity of TiO_2−FeO−Ti_2O_3−SiO_2−MgO−CaO−Al_2O_3 for high-titania slag smelting process [J]. Metallurgical and Materials Transactions B, 2018, 49(4): 1963−1973.
[24] ZHOU Fang-ming, XU Dong-hao, SHI Ming-xiao, BI Yan-hua. Investigation on microstructure and its transformation mechanisms of B_2O_3−SiO_2−Al_2O_3−CaO brazing flux system [J]. High Temperature Materials and Processes, 2020, 39: 88−95.
[25] CICEO-LUCACEL R, ARDELEAN I. FT-IR and Raman study of silver lead borate-based glasses [J]. Journal of Non-Crystalline Solids, 2007, 353: 2020−2024.
[26] XING Xiang-dong, DU Yue-li, ZHENG Jian-lu, WANG Sha, REN Shan, JU Jian-tao. Isothermal carbothermal reduction of $FeTiO_3$ doped with MgO [J]. JOM, 2021, 73(5): 1328−1336.
[27] XING Xiang-dong, PANG Zhuo-gang, ZHENG Jian-lu, DU Yue-li, REN Shan, JU Jian-tao. Effect of MgO and K_2O on high-Al silicon-manganese alloy slag viscosity and structure [J]. Minerals, 2021, 10(9): 810.
[28] WANG Zhen, SHU Qi-feng, CHOU Kuo-chih. Viscosity of fluoride-free mold fluxes containing B_2O_3 and TiO_2 [J]. Steel Research International. 2013, 84(8): 766−776.
[29] WANG Zhen, WANG Zhen, CHOU Kuo-chih. Study on structure characteristics of B_2O_3 and TiO_2-bearing F-free mold flux by Raman spectroscopy [J]. High Temperature Materials and Processes, 2013, 32(3): 265−273.
[30] WANG Zhen, CHOU Kuo-chih. Structure of CaO−B_2O_3−SiO_2−TiO_2 glasses: A Raman spectral study [J]. ISIJ International, 2011, 51(7): 1021−1027.
[31] URBAIN G. Viscosity estimation of slags [J]. Steel Research International, 1987, 58(3): 111−116.
[32] IIDA T, SAKAI H, KITA Y, SHIGENO K. An equation for accurate prediction of the viscosities of blast furnace type slags from chemical composition [J]. ISIJ International, 2000, 40(S): s110−s114.

B_2O_3 含量对 SiO_2−MgO−FeO 基熔渣黏度和结构的影响

张馨艺，李小明，邢相栋

西安建筑科技大学 冶金工程学院，西安 710055

摘　要：采用转筒法研究 B_2O_3 含量对 FeO−MgO−SiO_2 基渣系黏度的影响，利用 FTIR 分析方法研究不同 B_2O_3 含量下渣系结构的变化，并建立聚合度计算模型。结果表明，加入 B_2O_3 后熔体的黏度下降。当 B_2O_3 含量高于 3%(质量分数)时，B_2O_3 对熔体黏度的影响较小；随 B_2O_3 添加量由 0 增加至 4%(质量分数)，炉渣的熔化温度由 1152 ℃降低至 1050 ℃，表观活化能由 157.90 kJ/mol 降低至 141.84 kJ/mol。在熔融炉渣中加入 B_2O_3 破坏链状硅酸盐结构，形成更加环状的硼硅酸盐结构。采用修正的 Urbain 模型预测 SiO_2−MgO−FeO 基渣系黏度，实验得到的黏度值与新模型计算的黏度值吻合较好。

关键词：B_2O_3 含量；熔渣；黏度；活化能；结构

(Edited by Wei-ping CHEN)